Rotta, EH.; Marder, L.; Pérez-Herranz, V.; Moura Bernardes, A. (2021). Characterization of an anion-exchange membrane subjected to phosphate and sulfate separation by electrodialysis at overlimiting current density condition. Journal of Membrane Science. 635:1-9. https://doi.org/10.1016/j.memsci.2021.119510

Characterization of an anion-exchange membrane subjected to phosphate and sulfate separation by electrodialysis at overlimiting current density condition

Eduardo Henrique Rotta[1,2,*], Luciano Marder[1], Valentín Pérez Herranz[2], Andréa Moura Bernardes[1]

[1] LACOR, PPGE3M, Universidade Federal do Rio Grande do Sul, Av. Bento Gonçalves, 9500, 91509-900, Porto Alegre, RS, Brazil.

[2] IEC Group, ISIRYM, Universitat Politècnica de València, Camí de Vera s/n, 46022, València E-46071, Spain

* Corresponding author:

Eduardo Henrique Rotta

Av. Bento Gonçalves, 9500, Setor 4, Prédio 43426, Campus do Vale, 91509-900, Rio Grande do Sul, Brasil

E-mail: eduardo.rotta@ufrgs.br

Phone: +55 51 3308 9427.

Abstract: The structural degradation of an anion-exchange membrane used on the separation of phosphate from sulfate ions at overlimiting current density conditions was investigated. To this, the chemical structure changes, apparent counterion transport number, limiting current density, the apparent fraction of surface conductive regions, degree of hydrophobicity, membrane resistance and conductivity, morphology and thermal degradation profile were studied for the original and used samples of the anion-exchange membrane. The results showed that the degradation of the membrane fixed ion groups and structural polymer backbone affected the ionic transport conditions, reducing its apparent permselectivity and fraction of conductive regions. Also, the increase in the hydrophobicity degree together with the formation of cavities observed in the membrane surface may be responsible for the alteration of membrane conductivity, leading to a higher limiting current density value and a decrease in the plateau length.

Keywords: phosphate recovery, overlimiting conditions, ion-exchange membrane characterization, ionic transport properties, membrane deterioration

Highlights:

- Anion-exchange membrane was investigated before and after the separation process.
- Degradation of the membrane functional groups and polymer backbone was reported.
- The degraded membrane exhibited a lower counterion transport number.
- The plateau length was shortened by surface hydrophobization and cavities formation.
- The involvement of co-ions may cause an increase in water content in used membrane.

1. Introduction

The imminent phosphate rocks scarcity has fostered the need to remove and recover phosphorus from alternative sources, such as municipal wastewater [1,2]. In addition to controlling eutrophication, it is estimated that 15 to 20 % of global phosphate rock demand could be met through phosphorus recovery from municipal wastewater [3]. A well-studied and accepted technique for that purpose is precipitation/crystallization, in which the reaction between phosphate and calcium or magnesium compounds forms, respectively, hydroxyapatite [$Ca_5(OH)(PO_4)_3$] or struvite [$MgNH_4PO_4 \cdot 6H_2O$] [4]. However, its application is still challenging, since municipal wastewater usually reports a low P concentration, between 4 to 40 mg L^{-1}, together with the presence of coexisting ions, which may affect the induction time [5,6].

Electrodialysis can be considered an emerging alternative to overcome these limitations [7]. With little or no use of chemical reagents, this technology may allow the recovery of phosphate through the use of different experimental arrangements [8] and membranes with special characteristics [9,10]. Recently, a phosphate concentrated solution was obtained by an electrodialysis setup with 5 compartments operated in two stages [11]. In the first stage, the phosphate and coexisting ions of a solution simulating a municipal wastewater were concentrated up to a factor of 9.7 using a current density smaller than the limiting one ($i < i_{lim}$). Then, the phosphate ions were separated from sulfate and sodium ions by the usage of overlimiting conditions, in which the promoted intensive coupled effects of concentration polarization were able to suppress the transport of phosphate ions through the anion-exchange membrane by the formation of phosphoric acid (H_3PO_4) or PO_4^{3-} ions. This process was able to obtain a solution with a phosphate concentration higher than 100 mg L^{-1} and a low sulfate/phosphate ratio (approximately 2) – considered adequate by Liu et. al. [6]. However, this separation process conducted to significant alterations in the functional groups of the anion-

exchange membrane, with a transformation of the quaternary ammonium groups into tertiary amines.

Along with this, other membrane structure alterations may be reported, affecting its ionic transport conditions. Aging experiments with sodium hypochlorite [12] reported degradation of the quaternary ammonium groups of the membrane, together with a chain scission of its polymeric backbone throughout 700 h. After 2 years, Ghalloussi et. al. [13] observed the loss of functional sites of the anion-exchange membrane, decreasing its specific electrical conductivity. With experiments under intense current density regimes, Zabolotskiy et. al. [14] stated that the conversion of quaternary ammonium to tertiary/secondary amine groups promoted the water splitting reaction, altering the transport conditions of OH^- and salt ions. Also, it was observed a change in membrane resistance and permselectivity, and in the length of the plateau in polarization curves [15].

With the clarification of the mass transfer phenomena and mechanisms at $i > i_{lim}$ [16], the use of an intense current density value may enhance the transfer of ions [17] together with a decrease in the treatment time [18] and the effective area of the membrane, as well as promote the separation of ions with the same charge, such as phosphate and sulfate [11]. However, as mentioned before, it may affect the ion-exchange membrane attributes. In this context, the objective of this work is to evaluate the structural alterations of a commercial anion-exchange membrane subjected to the separation of phosphate and sulfate ions promoted at overlimiting conditions. Characterization techniques were conducted, and the properties of the original and used anion-exchange membrane were compared. From this, it is expected that a better understanding of the degradation process, as well as its influence on mass transport mechanisms, may help on the application and/or development of anion-exchange membranes that make viable the separation of phosphate from sulfate ions at overlimiting conditions, allowing the recovery of this important nutrient from municipal wastewater.

2. Experimental

The experiments to separate phosphate from sulfate ions were carried out with the same methodology used in Rotta et. al. [11]. A 5-compartment electrodialysis cell was employed, with 2 pairs of Chinese membranes with 16 cm^2 of effective area, supplied by Hidrodex®, alternately arranged to separate the compartments. The anion-exchange membrane, IONSEP-HC-A, contains quaternary ammonium groups as fixed ion-exchange sites, while the cation-exchange membrane, IONSEP-HC-C, has SO_3^- as attached sites. Both membranes have a heterogeneous structure, in which an ion-exchange resin containing the functional groups and fixed in a polymeric polyethylene matrix is pressed into a film form, reinforced by two nylon meshes [18,19]. As the anode and cathode of the cell, commercial Ti/70$TiO_2$30RuO_2 electrodes were used. Three reservoirs with 0.5 L were employed to feed the cell: the diluted reservoir received a solution with 0.116 g L^{-1} $Na_2HPO_4 \cdot 7H_2O$, 0.085 g L^{-1} $NaH_2PO_4 \cdot H_2O$, and 5.2 g L^{-1} Na_2SO_4; the concentrated and electrode reservoirs were filled with Na_2SO_4 solutions with 5.2 g L^{-1} and 8.0 g L^{-1}, respectively. The experiments were done in triplicate, at room temperature and galvanostatic mode for 4 h, applying a current density value of 25.0 mA cm^{-2} (corresponding to 125 % of the i_{lim}, previously obtained by polarization curves).

After this, the original and used anion-exchange membranes were characterized. Chemical structure changes, apparent counterion transport number, limiting current density and mass transport mechanisms, the apparent fraction of surface conductive regions, degree of hydrophobicity, membrane resistance and conductivity, morphology and thermal degradation profile were analyzed and compared.

To identify possible structural changes in the membrane, FTIR-HATR spectra were obtained. The sample preparation was similar to previous studies [11], where the membrane

was dried at 40 °C under a vacuum of 400 mmHg for 5 h and then kept in a desiccator for at least 48 h. The FTIR spectra were recorded by a Perkin Elmer Spectrum 1000 spectrophotometer after 32 scans between a wavenumber range of 4000-400 cm^{-1} and with a resolution of 4 cm^{-1}.

The apparent counterion transport number of the anion-exchange membrane was determined by the EMF method [20,21] using a 2-compartment electrodialysis cell at room temperature and in triplicate. Since this method also depends on the water transport across the membrane, the term "apparent counterion transport number" will be used to express the results. Before the analysis, a sample of the membrane with an effective area of 1 cm^2 was equilibrated at a 0.01 M NaCl solution for at least 24 h. After this, the sample was placed between the two compartments of the cell – one filled with a 0.05 M NaCl solution (C1) and the other with a 0.01 M NaCl solution (C2), both mechanically stirred. The membrane potential (E_m) was recorded for 1 h using two Ag/AgCl reference electrodes immersed in luggin capillaries, installed at each side of the membrane and connected at an Autolab PGSTAT302 potentiostat/galvanostat. The stationary value of E_m was recorded and employed to calculate the apparent counterion transport number (t_j^m) using Equation (1).

$$t_j^m = \left(\frac{1}{2}\right) \times \left(\frac{(E_m \times F)}{RT \times \ln\left(\frac{C1}{C2}\right)} + 1 \right) \quad (1)$$

where: F is the Faraday constant (96485.3 C mol^{-1}), R is the universal gas constant (8,314 J K^{-1} mol^{-1}) and T is the absolute temperature (298,15 K).

The limiting current density value and mass transport mechanisms were evaluated through polarization and chronopotentiometric curves. To this, chronopotentiometry experiments were conducted using a circular electrodialysis cell with 3 compartments, similar to that previously described and presented by Marder et. al. [22]. Each compartment was filled with 220 mL of a 0.025 M NaCl solution to avoid additional concentration gradients. A 3.14

cm^2 anion-exchange membrane was placed between anodic and diluted compartments. To minimize the effects of cathode reactions, a cation-exchange membrane separated the diluted and cathodic compartment. Both membranes were equilibrated with the 0.025 M NaCl solution for at least 24 h. The current was imposed by the potentiostat/galvanostat plugged between 2 graphite electrodes in a range of 0.001 – 0.030 A, and the potential value of the anion-exchange membrane was monitored by the reference electrodes. A pre-established value of current (i) was applied for 120 s and the membrane potential value (U_m) was automatically measured. After this, a system diffusion relaxation time (120 s) was carried out and recorded before the next value of current. The polarization curves were obtained by plotting each applied value of i versus U_m, considering the value of membrane potential right before relaxation time. In turn, the chronopotentiometric curves were represented by U_m versus experimental time for each value of current.

The fraction of surface conductive regions was calculated using Equation (2). This is a Sand modified equation proposed by Choi and Moon [23,24] to include the heterogeneity of ion-exchange membranes, considering the current line perpendicular to the membrane surface and an infinitely large diffusion layer – normally not met. In heterogeneous surfaces, this 1D model may present some inconsistency, since it does not consider the deviations of current lines occurred [25], which may condense in the conductive regions and create a funneling effect [26]. Regarding the analysis of chronopotentiometric results, this model still gives valuable information. When high values of current density are applied ($i > 1.5i_{lim}$ for homogeneous membranes [25]), the solution mixing by convective vortices in the membrane/solution interface should comply with the Sand theory of infinitely large diffusion layer. In heterogeneous membranes, the appearance of a second transition time (attributed to the time when critically low values of concentration are reached at the whole surface of the membrane, i.e., conductive and non-conductive region) may be equivalent to the Choi-Moon transition time

[27]. Thus, the fraction of conductive area determined is called "apparent fraction of surface conductive area" (ε), and only the values of the second transition time for values of $i > 1.5i_{lim}$ are considered. The values were plotted versus i^{-2}, obtaining a linear correlation passing through the origin ($y = \alpha \times x + \beta$, with $\beta = 0$), where the slope of the curve was used to obtain ε when knowing the t_j^m values from Equation (1).

$$\tau = \left(\frac{\pi \times D}{4}\right) \times \left(\frac{\varepsilon \times z \times F \times C_0}{t_j^m - t_j^s}\right)^2 \times \left(\frac{1}{i}\right)^2 \quad (2)$$

where D is the diffusion coefficient of NaCl solution (1.609×10^{-5} cm^2 s^{-1}), z is the counterion charge, C_0 is the salt concentration in the solution (0.025 M) and t_j^s (0.604) is the transport number of Cl^- ions in the solution phase [28].

The degree of hydrophobicity of the membrane was determined by measuring the contact angle by the sessile drop method. A drop of water of approximately 3 µL was deposited at a vertical distance of 0.7 cm using the Drop Shape Analyzer (Kruss®, DSA30). Before the analysis, excess water was removed from the membrane with filter paper [29], immobilizing it on a platform in the flat position. The images of at least 8 depositions of droplets spread horizontally on the membrane surface were captured with a high-resolution camera and then imported in the Surftens software to determine the value of the contact angle [30]. The measurements were made at room temperature and in triplicate.

The membrane resistance and conductivity were accomplished on an impedance analyzer (Solartron®, 1260), at a scan frequency range of 1 Hz and 10 µHz. Before the experiments, the membranes were equilibrated in a solution of 0.01 M NaCl for 24 hours. The membrane sample was fixed between two stainless steel electrodes, with a distance of 0.916 cm, and inserted into the electrochemical cell at a temperature of 20 °C and relative humidity of 100% [31]. With the Zplot® software, the data were represented in the Nyquist plot, where the value of membrane resistance (R_m) is obtained from the real impedance value when the

185 imaginary part is equal to zero [32]. Then, the membrane conductivity value (k_m, S cm^{-1}) may
186 be calculated with Equation (3), being a function of membrane area (A, cm^2) and resistance
187 (R_m, Ω), as well as the distance between both electrodes (d, cm).

$$k_m = \frac{d}{R_m \times A} \quad (3)$$

188 The analysis of morphology and relief of the membrane was carried out using a scanning
189 electron microscope (Phenon ProX), operated at 10 kV. To prevent any surface modification,
190 the membrane was arranged in a sample holder without metallization.
191 The thermal degradation profile of the anion-exchange membrane was obtained using a
192 Thermogravimetric Analyzer (TA Instruments, Q50). The sample was heated from room
193 temperature up to a maximum of 940 °C at a rate of 20 °C min^{-1} in a controlled N_2 atmosphere.
194

195 **3. Results and Discussion**

196

197 The electrodialysis results presented a similar behavior to the observed in Rotta et. al.
198 [11] and can be seen in the Supplementary Materials. As expected, the use of electrodialysis at
199 overlimiting current density restricted the transport of phosphate ions through the ion-exchange
200 membrane after the first hour of experiments (see Figure S1 and Figure S2), allowing its
201 separation from sulfate ions. Such current density condition may boost coupled effects of
202 concentration polarization at the interface between the anion-exchange membrane and diluted
203 solution (evidenced by the increase in membrane potential, Figure S3), leading to the generation
204 of H^+ and OH^- from water splitting, together with the protonation-deprotonation of phosphate
205 species. However, this condition causes a degradation in the functional groups of the anion-
206 exchange membrane, as briefly presented by FTIR/ATR spectra in the previous study.
207 New spectra obtained in the presented work also indicated a possible deterioration of
208 the structural mesh of the membrane. Divided into six main regions, Figure 1 presents the

FTIR/ATR spectra for samples of (a) original and (b) used anion-exchange membrane. The absorption peaks presented in regions (1), (3), and (6) are similar for both membrane samples. They may be attributed to the ν stretches (region 1, peaks at 2915 and 2845 cm^{-1}) and δ deformations (peaks at 1465 cm^{-1} and 718 cm^{-1} in regions 3 and 6, respectively) of the C-H bonds of its polymeric polyethylene matrix. The absorption peak at 1715 cm^{-1} in the region (2), reported only for the original membrane, may refer to the ν(C=O) stretching vibrations present in the nylon meshes, used as structural reinforcement. The absence of this peak in the used membrane spectrum may indicate structural changes in this mesh resulting from hydrolysis reactions in the C-N-C bonds, catalyzed by the reduction of pH values in the membrane/diluted solution interface and/or the increase in pH in the solution presented in the concentration compartment [33] – as presented by Figure S4 of the Supplementary Materials. According to Garcia-Vasquez et. al. [34], this could explain the change in the coloration of the membrane after its usage to separate phosphate and sulfate ions, reported in Rotta et. al. [11].

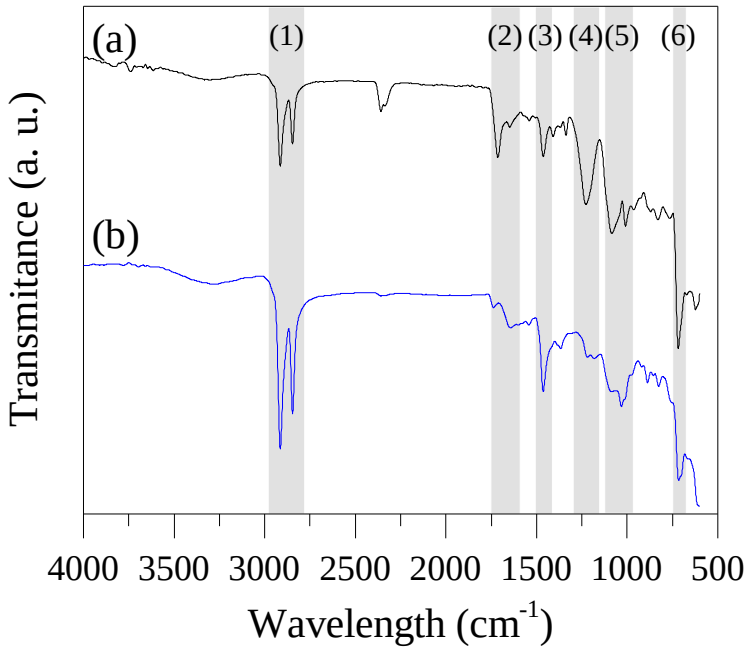

Figure 1. FTIR spectra for (a) original and (b) used anion-exchange membrane. Region (1), (3) and (6) are related to the ν stretches (peaks at 2915 and 2845 cm^{-1}) and δ deformations (peaks at 1465 cm^{-1} and 718 cm^{-1}) of the C-H bonds of membrane polymeric polyethylene matrix. Region (2) refers to the ν(C=O) stretching vibrations (peak at 1715 cm^{-1}) of structural reinforcement nylon meshes. Region (4) with a peak at 1230 cm^{-1} is related to the quaternary ammonium groups. Region (5) may be associated with tertiary amine groups, peak at 1050 cm^{-1}.

223

224 The differences between the original and used membrane can also be noted in regions
225 (4) and (5), associated with the membrane functional groups. The spectra of the original
226 membrane presented a peak at 1230 cm^{-1} (region 4), related to the quaternary ammonium groups
227 of the anion-exchange membrane [12]. For the used membrane, the peak at this wavelength was
228 suppressed and a new peak at 1050 cm^{-1} in the region (5) was detected, indicating that original
229 functional groups ($–NR_3^+$) were partially transformed into tertiary amine groups in the
230 membrane structure [15]. As mentioned before, the hydrolysis of the functional groups was also
231 observed in Rotta et. al. [11], and may be due to the direct action of OH^- ions produced in the

water splitting reaction and protonation/deprotonation of phosphate species. Although it is known that the protonation/deprotonation reaction may occur also at underlimiting current density conditions when working with ampholyte-containing solutions [35], the high electric field applied to successfully promote the separation of phosphate from sulfate ions may intensify this reaction, together with the coupled effects of concentration polarization (such as water splitting) [15,36,37], and indirectly affect the degradation of the functional groups. It is important to highlight that the uncertainties about the commercial anion-exchange membrane baseline materials, such as the ion-exchange resin of the IONSEP-HC-A, prevent the prediction of the specific degradation mechanism [38], which can be by the Hofmann elimination (or E2 elimination), nucleophilic substitution (S_N2 mechanism), E1 elimination as well as other degradation routes [38–41].

As discussed before, these structural changes may significantly influence the conditions of ionic transport through the membrane. To complement this information, the apparent counterion transport number was firstly evaluated. This parameter may be defined as the total current density fraction carried by the counterions crossing the membrane [42], ideally equal to 1. Using Eq. 1, the apparent counterion transport number (t_j^m) of the original membrane reported an average value of 0.996 ± 0.001, whereas for the used membrane an average t_j^m = 0.934 ± 0.001 was obtained. The reduction of this parameter for the used membrane may indicate an increase in the current density fraction carried by co-ions and an increase in water transport across the membrane.

The presence of parallel reactions such as water dissociation in the membrane/solution interface may also affect counterion transport number values. According to Simons' catalytic theory [43,44], weakly-based functional groups, such as tertiary amines, have a catalytic effect on water dissociation via reversible protonation and deprotonation reactions, presented in Equations (4) and (5), with B as a weak base.

$$B + H_2O \leftrightarrow BH^+ + OH^- \quad (4)$$

$$BH^+ + H_2O \leftrightarrow B + H_3O^+ \quad (5)$$

Wang et. al. [45] point out that this is observed due to the lower ion-exchange capacity of these functional groups. As a result of an unsatisfactory current density conduction demand, the authors affirm that water dissociation takes place and lower limiting current density (i_{lim}) values are reported. Choi and Moon [15] also state that the OH^- ions generated in the water dissociation may neutralize the tertiary amine groups present in the internal solution of the membrane, contributing to the reduction of the i_{lim} value and the extension of the plateau observed in polarization curves.

A typical polarization curve can be divided into three well-defined regions [35]. The first region shows a linear dependence between current density and potential values in a quasi-ohmic behavior, the second region is defined by an inclined plateau associated with a limiting state, and the third region is associated with overlimiting mass transfer mechanisms, such as water splitting and electroconvection. Despite presenting a conventional shape, the polarization curves (Figure 2) obtained in the present study showed different behavior in terms of i_{lim} values and plateau length. As can be seen in Figure 2(a), the original membrane presented an $i_{lim,AEM}$ value of 2.142 mA cm^{-2}, while the used membrane (Figure 2(b)) reported an $i_{lim,AEM}$ = 2.396 mA cm^{-2}. Also, a decrease in the plateau extension of the used membrane is observed, which means that mass transfer mechanisms related to the third region of the polarization curve are reached at a lower potential value, approximately 2.242 V, against 2.631 V of the original membrane. The catalytic effect of tertiary amine groups in the water dissociation may have a contribution in reducing the plateau length, but it would not explain the increase in the i_{lim} values – discussed together with the results of chronopotentiometric curves.

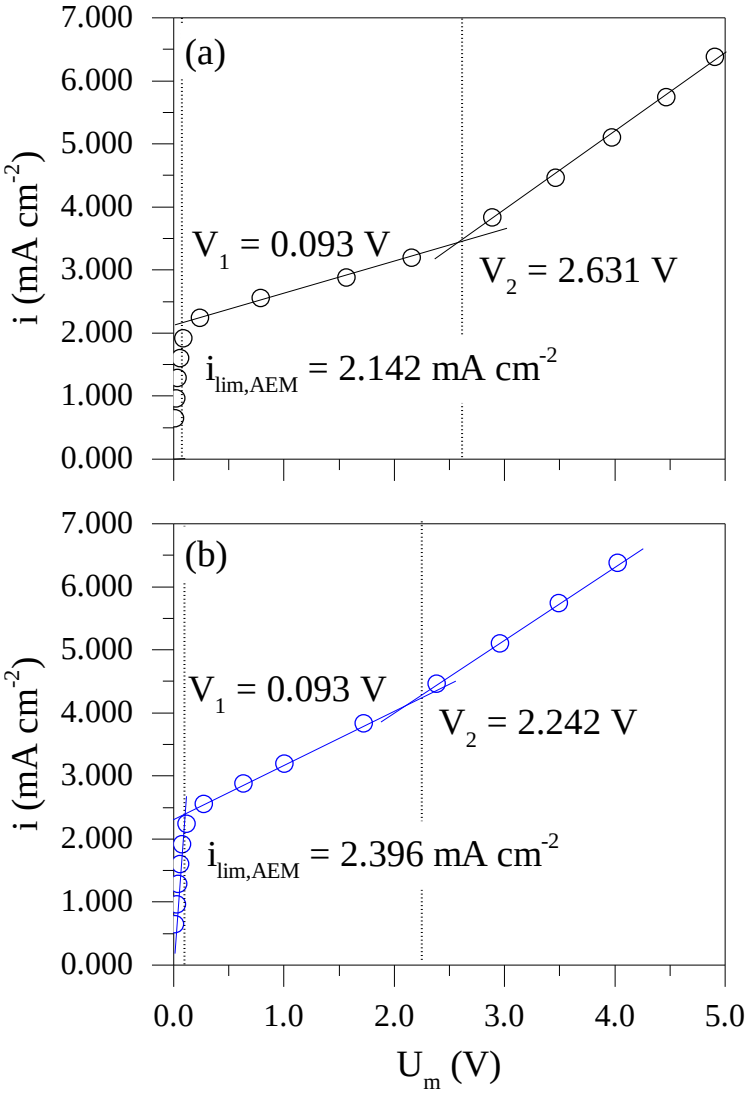

Figure 2. Polarization curves for (a) original and (b) used anion-exchange membrane

279

280 The chronopotentiometric curves for the original and used membrane are shown in
281 Figure 3. For both membranes, at $i < i_{lim}$, the chronopotentiometric curves presented a similar
282 shape, characteristic of heterogeneous ion-exchange membranes [46]. With the increase of the
283 applied current value, the appearance of inflection points as a result of the concentration
284 polarization, characteristic of chronopotentiometric curves at $i > i_{lim}$, can be observed. The
285 presence of these inflection points occurred at different current values for both membranes, in
286 agreement with the polarization curves data. For the original sample of the membrane, Figure
287 3(a), an inflection point at current values ≥ 0.008 A (corresponding to 2.548 mA cm^{-2}) can

already be noted, while for the used membrane (Figure 3(b)) this behavior is only observed for values ≥ 0.010 A (or 3.185 mA cm^{-2}).

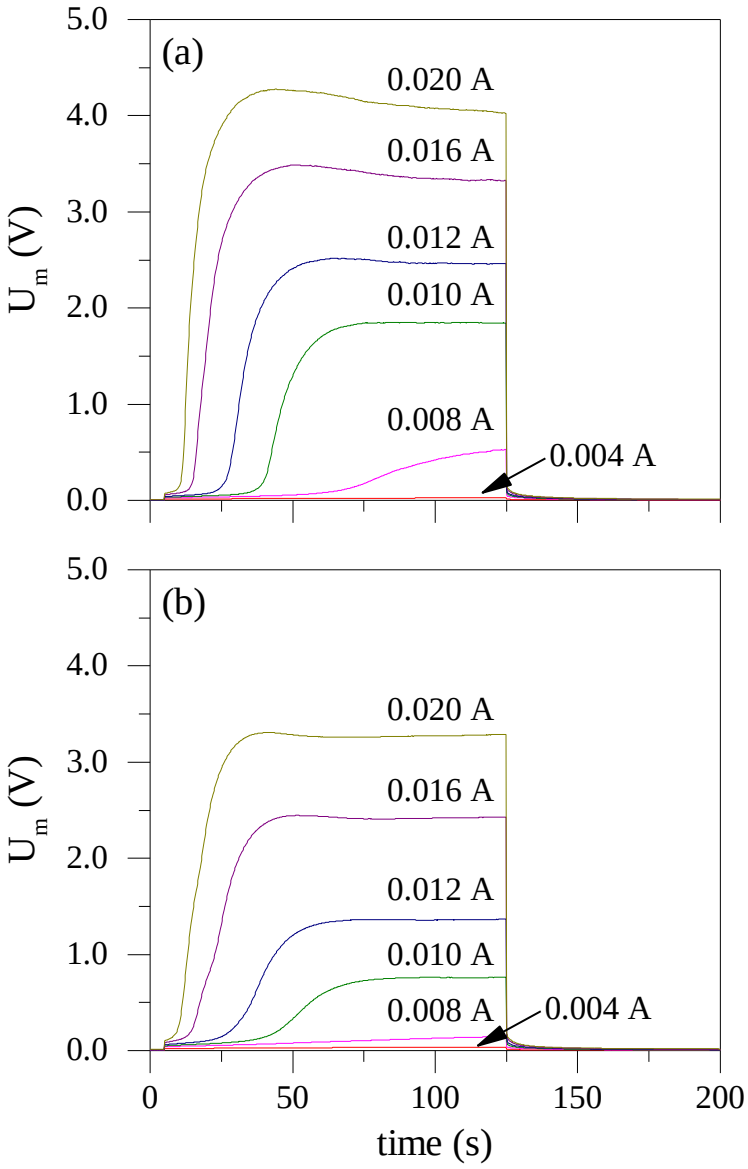

Figure 3. Chronopotentiometric curves for (a) original and (b) used anion-exchange membrane

The format of chronopotentiometric curves at $i > i_{lim}$ values may provide important information about the overlimiting mass transport mechanisms [47]. For both membrane samples, a maximum U_m value was observed after the inflection point (most evident in Figure

3(a)), decreasing its values along the time until reaching a stationary state. Gally et. al. [48] attributed this behavior to the formation of new ionic species at the membrane/solution interface, as well as to the transfer of co-ions across the membrane, indicating the presence of water splitting and loss of permselectivity. The absence of a plateau after the current switch off indicated no fouling and/or bipolar character of the membrane [22].

From the transition time (τ) data of the obtained chronopotentiometric curves at overlimiting conditions, the apparent fraction of surface conductive regions (ε) was calculated from the linearizing curves shown in Figure 4.. Considering a slope (α) value of 391.73, the original membrane presented an apparent fraction of conductive regions of 0.905, that is, one can consider that 90.50 % of the apparent membrane surface area is composed of ion-exchanging sites. This value is consistent with the obtained by Nagarale et. al. [50], Kim et. al. [51] and Martí-Calatayud et. al. [52] for anion- and cation-exchange membranes with different degrees of functionalization. For the used membrane, the linearized curve presented a higher slope (α = 421.42), which may be translated to a reduction in the apparent degree of functionalization to values of approximately 79.01 %. This behavior may be associated with elimination mechanisms that may take place, as well as a possible neutralization of tertiary amine groups by OH^- generated by water splitting, as already discussed.

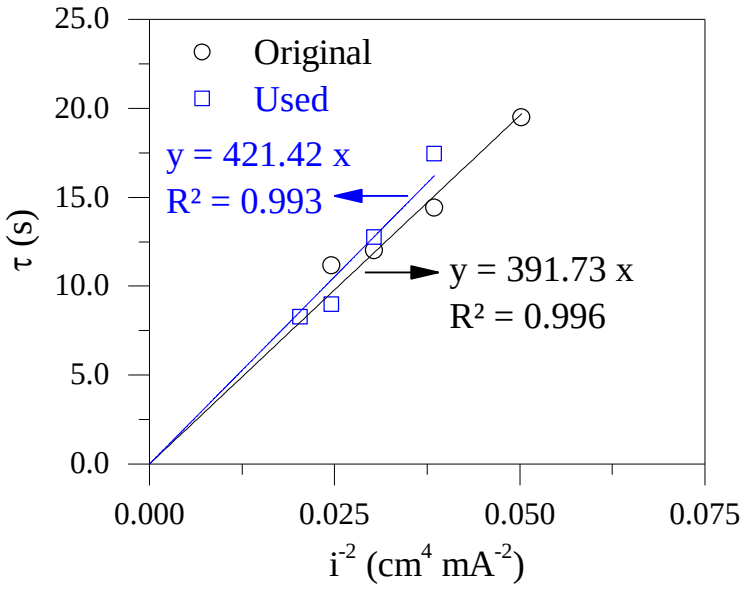

Figure 4. $\tau \times i^{-2}$ linearization curves for original (black line) and used (blue line) anion-exchange membrane

313

314 Ideally, a lower ε value would result in a reduction of the i_{lim} and an extension in the
315 plateau of polarization curves [45], which was not reported in this study. This behavior may be
316 associated with three main factors related to the membrane [53–56]. The first is the loss of
317 permselectivity (directly related to the reported decrease in the apparent transport number), with
318 the diffusion and electromigration of co-ions across the membrane delaying the polarization
319 limiting state and, consequently, increasing the i_{lim} value. The second one, the degree of
320 hydrophobicity, may influence the ionic transfer rate, since with higher degrees of
321 hydrophobicity, there will be lower attraction forces between the solution and membrane,
322 reducing the slow-down effect and facilitating the flow of ions [53,56]. The third is the
323 formation of cavities or undulations in micrometric scales on the membrane surface, which may
324 promote and/or intensify the formation of electroconvective vortices, responsible for renewing
325 the scarce ion solution at the membrane/solution interface, at lower voltage values –
326 diminishing the plateau length. It is important to note that possible water splitting at the
327 interface between membrane and solution may cause disturbances and/or weaken the presence

328 of these electroconvective vortices, given the formation of additional charge carriers (H^+ and
329 OH^- ions) in this region [57].

330 To evaluate the degree of hydrophobicity of the membrane, contact angle (θ)
331 experiments were conducted. As can be seen in Figure 5, the used membrane presented a higher
332 hydrophobicity character, with an average contact angle value of (87.27 ± 1.13) °, compared to
333 the original membrane, which reported an average θ = (80.81 ± 1.68) °. This change in the
334 hydrophobicity degree may be related to the degradation of the functional conductive groups
335 of the membrane, and the consequent removal of its surface by the solution flow [53]. Thus, the
336 fraction of a relatively hydrophobic polymer on the membrane surface is increased together
337 with the degree of hydrophobicity, facilitating the ionic flow as mentioned before.
338

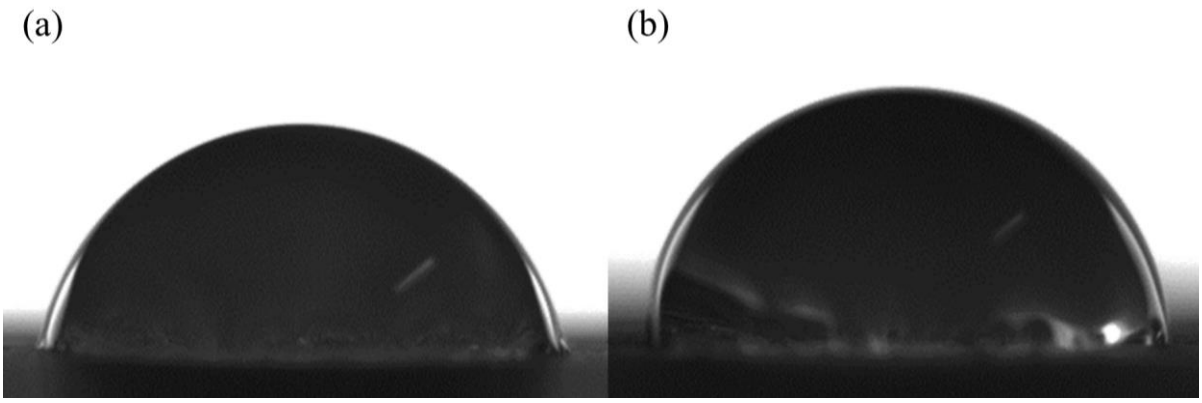

Figure 5. The contact angle of (a) original and (b) used anion-exchange membrane

339

340 Regarding the formation of cavities on the membrane surface, scanning electron
341 microscopy (SEM) images were obtained. Figure 6 shows different SEM images of the original
342 and used membrane surface at 500x and 1000x of magnification, where can be observed its
343 heterogeneity with the random distribution of conductive areas in a non-conductive polymeric
344 matrix. In SEM images of the original membrane presented in Figure 6(a-b), small irregularities
345 near the functional groups are observed, probably associated with the manufacturing process.

However, when the SEM images of the used membrane are analyzed (Figure 6(c-d)), it can be noted several holes and cavities on the membrane surface and the worsening of irregularities inherent to the fabrication process. This behavior may be associated with the exposure of the membrane to high current density values and a possible temperature increase at the membrane/solution interface [12,34,58]. Although is difficult to determine the temperature in this interface, Choi and Moon [15] affirm that an increase in the temperature solution is inherent to the electrodialysis treatment. Also, the authors report that this process may be intensified when operating at overlimiting current density conditions, considering the relation between the Joulean heat and the remarkably high field strength present in the membrane/solution interface.

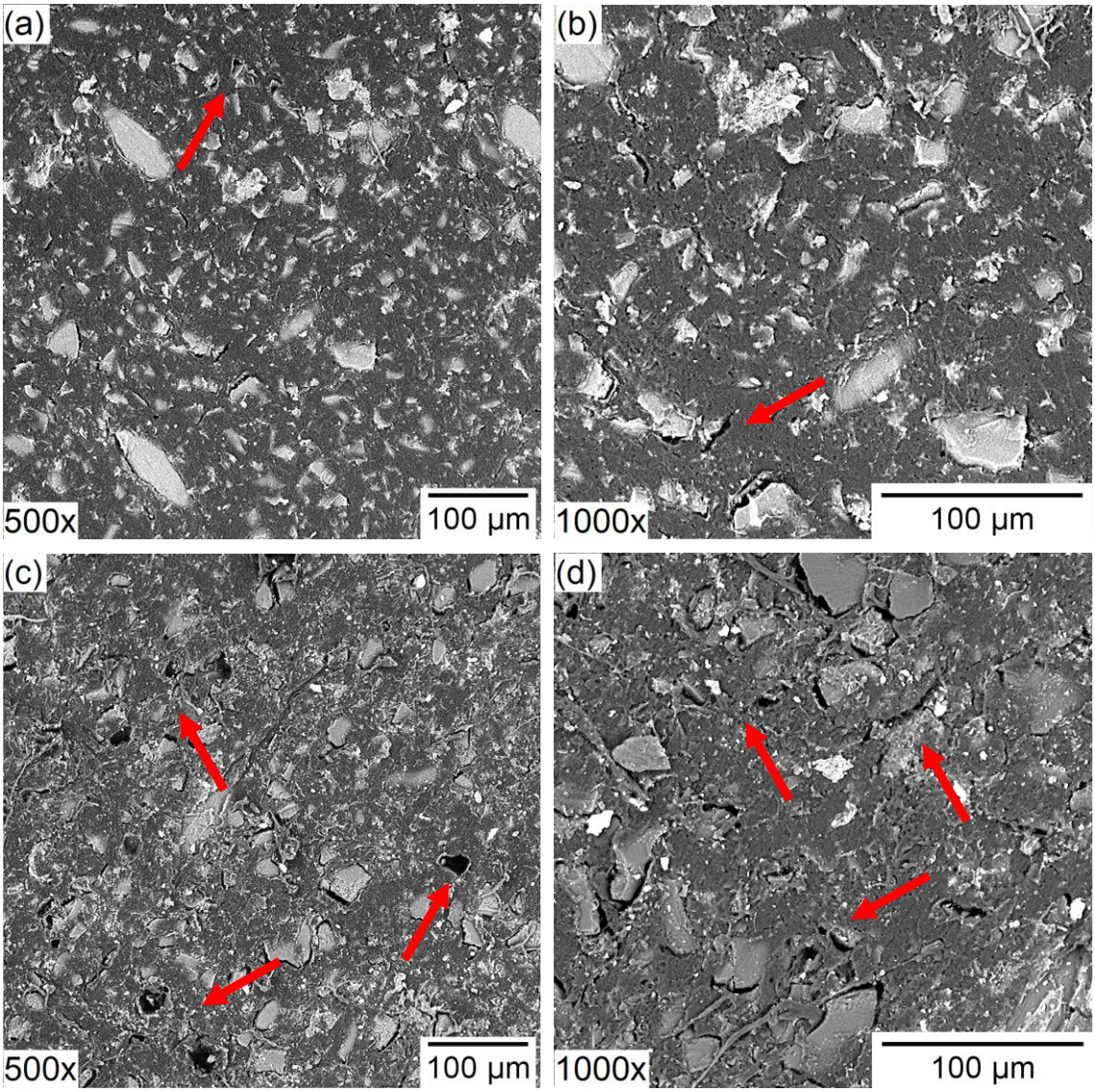

Figure 6. Scanning electron microscopy images of the surface of (a-b) original and (c-d) used anion-exchange membrane 500x and 1000x of magnification

355

356 The presence of these cavities can directly influence the ion-exchange membrane
357 resistance and conductivity. Garcia-Vasquez et. al. [12] reported an increase in the value of
358 conductivity of homogeneous anion- and cation-exchange membrane (AMX and CMX,
359 respectively) and heterogeneous MK40 membrane after 100 h of exposure to a sodium
360 hypochlorite solution. The authors attributed this behavior to the formation of cavities and holes
361 due to the polymer chain scissions, which are a result of the subtraction of the polymer backbone

α-hydrogen by hydroxyl radicals. These imperfections may increase the intergel fraction of the membrane, allowing higher external electrolyte solution permeability and co-ions sorption, to the detriment of permselectivity and the Donnan Exclusion effect [59,60].

The resistance (R_m) of the original and used IONSEP-HC-A membrane was determined by electrochemical impedance spectroscopy experiments, presented in Figure 7, and its conductivity (k) was calculated using Equation (3). The original anion-exchange membrane showed an average electrical resistance of (4.30 ± 0.03) kΩ, equivalent to an average electrical conductivity value (k) of (3.53 ± 0.04) mS cm^{-1} – value in accordance with the obtained by Bhadja et. al. [61]. In turn, the used membrane reported a relatively lower average electrical resistance value, R_m = (3.19 ± 0.13) kΩ and, consequently, a higher average conductivity, k = (4.40 ± 0.19) mS cm^{-1}. This difference confirms the influence of cavities in the polymeric matrix of the membrane on its electrical conductivity behavior. Another hypothesis to the increase in membrane conductivity is the ampholyte nature of the solution, reported by Sarapulova et. al. [36]. With the increase in OH^- in the internal solution of the membrane due to associated effects of concentration polarization, the singly charged phosphate species may be transformed to the double charged species in the membrane bulk solution, increasing its conductivity values.

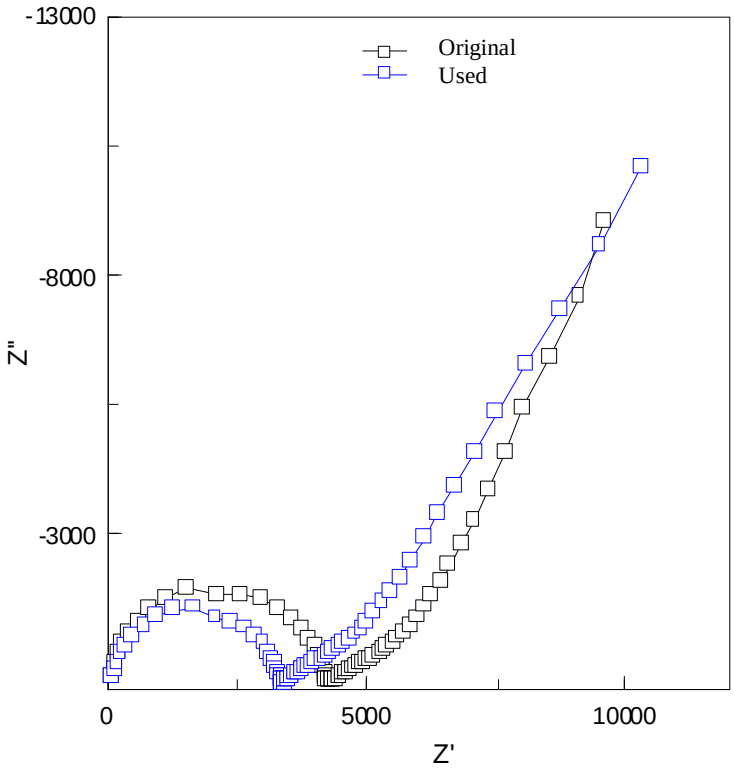

Figure 7. Nyquist plots of original (black line) and used (blue line) anion-exchange membranes

379

380 Also, the thermal-oxidative stability of the membrane was evaluated through
381 thermogravimetric analysis (TGA). As can be seen in Figure 8, both membrane samples
382 presented three mass-loss events. Concerning the original membrane (Figure 8(a)), the first
383 event occurred at temperatures below 100 °C may refer to the evaporation of membrane water
384 content [62], and represented an average mass loss of (32.50 ± 2.15) %. The second event,
385 between a range of temperatures of 200 °C – 340 °C and with an average mass loss of (13.10 ±
386 0.20) %, is related to the degradation of the functional groups of the ion-exchange membrane
387 [12]. The third event, responsible for the main amount of mass loss, an average value of (50.24
388 ± 1.95) %, occurred at temperatures higher than 340 °C and may be linked to the degradation
389 of the polymeric matrix [63]. The mass loss events of the used membrane were reported at
390 similar temperature ranges, with (38.91 ± 1.06) % of average mass loss linked to water

391 evaporation, (11.51 ± 0.20) % to the functional group degradation and (43.62 ± 0.37) % related
392 to the polymeric matrix.
393

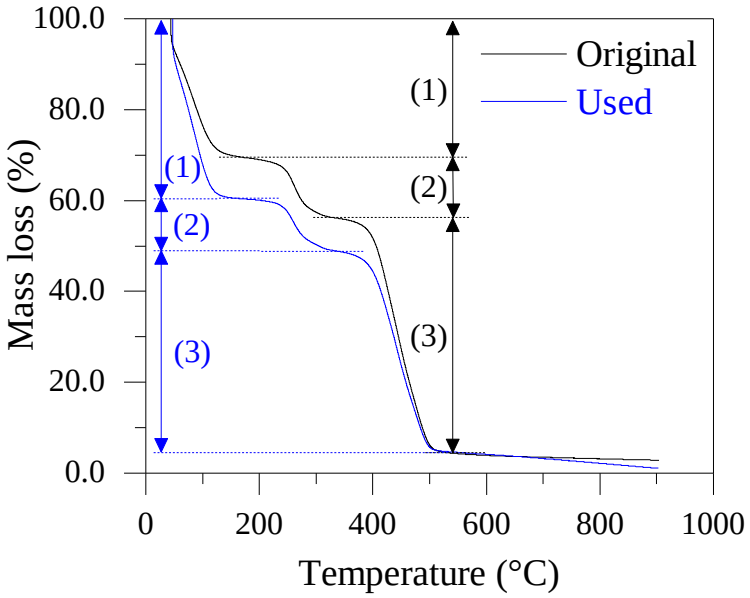

Figure 8. Thermogravimetric curves of (a) original and (b) used anion-exchange membrane. The first event (1) is related to the evaporation of membrane water content. The second event (2) may be linked to the degradation of functional groups. The third event (3) is associated to the degradation of the membrane polymeric matrix.

394

395 Comparing both membranes, it can be noted slight changes in the values of TGA events.
396 The increase in used membrane water content, despite presenting a higher degree of
397 hydrophobicity, may be related to the involvement of co-ions [64]. The increase in intergel
398 fraction with the presence of external electrolyte solution in cavities may impacts the
399 permselectivity and Donnan Exclusion effect, as already reported, and the sorption of co-ions
400 may contribute to increasing the water content and membrane thickness, which increased from
401 (0.705 ± 0.002) mm to (0.758 ± 0.003) mm. Regarding the functional groups and polymeric
402 matrix deterioration, the decrease in its values may be linked to the alteration of the structural

mesh of the used membrane, in addition to the formation of cavities on its surface. Also, it is important to note the presence of approximately 2 % of mass residues on the TGA curve of the original membrane, a condition that may be related to the presence of non-volatile inorganic ions in the membrane structure, probably due to the manufacturing process [65]. A simple equilibration of the membrane with the working solution can mitigate this effect.

The degradation of the IONSEP-HC-A membrane structure hindered its performance and application in the separation of phosphate from sulfate ions at $i > i_{lim}$. The stability at high pH values generally presented by anion-exchange membranes is a constant challenge also in AEM electrolyzer operation [41,66], and significant advances have already been achieved by studying different types of reinforcement materials, polymer backbone, and the use of inorganic nanocomposites in the membrane structure [67–69]. In this bias, future studies may focus on the application and/or development of alkali-resistant anion-exchange membranes suitable for the separation of phosphate and sulfate ions at overlimiting conditions.

4. Conclusions

Through the separation of phosphate and sulfate at overlimiting conditions, the results showed not only a degradation of the membrane functional groups, but also in its structural mesh and polymeric matrix. These events impacted the transport properties of the membrane, reducing its apparent permselectivity, as well as stimulating coupled effects of concentration polarization at the membrane/solution interface. The relation between apparent conductive region fractions, limiting current density value, and the length of the plateau of polarization curves presented a tendency contrary to the literature, which may be linked to an increase in the degree of hydrophobicity and the formation of holes/cavities in the polymeric matrix. These

events may restrict the anion-exchange membrane lifetime, as well as its applicability in phosphate/sulfate separation at overlimiting conditions.

Acknowledgments

The authors are grateful for the research grant funded by Coordenação de Aperfeiçoamento de Pessoal de Nível Superior – CAPES/Brazil (88882.345780/2010-01). The financial support of the Brazilian funding agencies Conselho Nacional de Desenvolvimento Científico e Tecnológico – CNPq/Brazil, Fundação de Amparo à Pesquisa do Estado do Rio Grande do Sul FAPERGS/Brazil, Financiadora de Estudos e Projetos -FINEP/Brazil, and from the Ibero-American Program on Science and Technology for Development (CYTED) are also acknowledged. Moreover, this project was founded by CNPq (CNPq/BRICS-STI-2-442229/2017-8), RFBR (No. 18-58-80031), DST (DST/IMRCD/BRICS/PC2/From waste to resources/2018 (G)), NSFC (51861145313), NRF (No: 116020).

References

[1] Y. Wu, J. Luo, Q. Zhang, M. Aleem, F. Fang, Z. Xue, J. Cao, Potentials and challenges of phosphorus recovery as vivianite from wastewater: A review, Chemosphere. 226 (2019) 246–258. https://doi.org/10.1016/j.chemosphere.2019.03.138.

[2] O. Larriba, E. Rovira-Cal, Z. Juznic-Zonta, A. Guisasola, J.A. Baeza, Evaluation of the integration of P recovery, polyhydroxyalkanoate production and short cut nitrogen removal in a mainstream wastewater treatment process, Water Research. 172 (2020) 115474. https://doi.org/10.1016/j.watres.2020.115474.

[3] Z. Yuan, S. Pratt, D.J. Batstone, Phosphorus recovery from wastewater through microbial processes, Current Opinion in Biotechnology. 23 (2012) 878–883. https://doi.org/10.1016/j.copbio.2012.08.001.

[4] Y. Ye, H.H. Ngo, W. Guo, Y. Liu, J. Li, Y. Liu, X. Zhang, H. Jia, Insight into chemical phosphate recovery from municipal wastewater, Science of The Total Environment. 576 (2017) 159–171. https://doi.org/10.1016/j.scitotenv.2016.10.078.

[5] M. Xie, H.K. Shon, S.R. Gray, M. Elimelech, Membrane-based processes for wastewater nutrient recovery: Technology, challenges, and future direction, Water Research. 89 (2016) 210–221. https://doi.org/10.1016/j.watres.2015.11.045.

[6] Y. Liu, X. Sheng, Y. Dong, Y. Ma, Removal of high-concentration phosphate by calcite: Effect of sulfate and pH, Desalination. 289 (2012) 66–71. https://doi.org/10.1016/j.desal.2012.01.011.
[7] L. Gurreri, A. Tamburini, A. Cipollina, G. Micale, Electrodialysis Applications in Wastewater Treatment for Environmental Protection and Resources Recovery: A Systematic Review on Progress and Perspectives, Membranes. 10 (2020) 146. https://doi.org/10.3390/membranes10070146.
[8] P. Guedes, E.P. Mateus, J. Almeida, A.R. Ferreira, N. Couto, A.B. Ribeiro, Electrodialytic treatment of sewage sludge: Current intensity influence on phosphorus recovery and organic contaminants removal, Chemical Engineering Journal. 306 (2016) 1058–1066. https://doi.org/10.1016/j.cej.2016.08.040.
[9] R. Liu, Y. Wang, G. Wu, J. Luo, S. Wang, Development of a selective electrodialysis for nutrient recovery and desalination during secondary effluent treatment, Chemical Engineering Journal. (2017). https://doi.org/10.1016/j.cej.2017.03.149.
[10] A.T.K. Tran, Y. Zhang, J. Lin, P. Mondal, W. Ye, B. Meesschaert, L. Pinoy, B. Van der Bruggen, Phosphate pre-concentration from municipal wastewater by selectrodialysis: Effect of competing components, Separation and Purification Technology. 141 (2015) 38–47. https://doi.org/10.1016/j.seppur.2014.11.017.
[11] E.H. Rotta, C.S. Bitencourt, L. Marder, A.M. Bernardes, Phosphorus recovery from low phosphate-containing solution by electrodialysis, Journal of Membrane Science. 573 (2019) 293–300. https://doi.org/10.1016/j.memsci.2018.12.020.
[12] W. Garcia-Vasquez, R. Ghalloussi, L. Dammak, C. Larchet, V. Nikonenko, D. Grande, Structure and properties of heterogeneous and homogeneous ion-exchange membranes subjected to ageing in sodium hypochlorite, Journal of Membrane Science. 452 (2014) 104–116. https://doi.org/10.1016/j.memsci.2013.10.035.
[13] R. Ghalloussi, W. Garcia-Vasquez, L. Chaabane, L. Dammak, C. Larchet, S.V. Deabate, E. Nevakshenova, V. Nikonenko, D. Grande, Ageing of ion-exchange membranes in electrodialysis: A structural and physicochemical investigation, Journal of Membrane Science. 436 (2013) 68–78. https://doi.org/10.1016/j.memsci.2013.02.011.
[14] V.I. Zabolotskiy, A.Yu. But, V.I. Vasil'eva, E.M. Akberova, S.S. Melnikov, Ion transport and electrochemical stability of strongly basic anion-exchange membranes under high current electrodialysis conditions, Journal of Membrane Science. 526 (2017) 60–72. https://doi.org/10.1016/j.memsci.2016.12.028.
[15] J.-H. Choi, S.-H. Moon, Structural change of ion-exchange membrane surfaces under high electric fields and its effects on membrane properties, Journal of Colloid and Interface Science. 265 (2003) 93–100. https://doi.org/10.1016/S0021-9797(03)00136-X.
[16] V.V. Nikonenko, A.V. Kovalenko, M.K. Urtenov, N.D. Pismenskaya, J. Han, P. Sistat, G. Pourcelly, Desalination at overlimiting currents: State-of-the-art and perspectives, Desalination. 342 (2014) 85–106. https://doi.org/10.1016/j.desal.2014.01.008.
[17] M.C. Martí-Calatayud, M.S.-C. Poczatek, V. Pérez-Herranz, Trade-Off between Operating Time and Energy Consumption in Pulsed Electric Field Electrodialysis: A Comprehensive Simulation Study, (2021) 15.
[18] S.D. Bittencourt, L. Marder, T. Benvenuti, J.Z. Ferreira, A.M. Bernardes, Analysis of different current density conditions in the electrodialysis of zinc electroplating process solution, Separation Science and Technology. (2017) 1–11. https://doi.org/10.1080/01496395.2017.1310896.
[19] M.C. Martí-Calatayud, E. Evdochenko, J. Bär, M. García-Gabaldón, M. Wessling, V. Pérez-Herranz, Tracking homogeneous reactions during electrodialysis of organic acids via EIS, Journal of Membrane Science. 595 (2020) 117592. https://doi.org/10.1016/j.memsci.2019.117592.

[20] M. Ottay, T. Frarland, S.K. RatkJe, S. Moller-Holst, Membrane transference numbers from a new emf method, (1992) 8.
[21] M.I. Khan, A.N. Mondal, B. Tong, C. Jiang, K. Emmanuel, Z. Yang, L. Wu, T. Xu, Development of BPPO-based anion exchange membranes for electrodialysis desalination applications, Desalination. 391 (2016) 61–68. https://doi.org/10.1016/j.desal.2015.11.024.
[22] L. Marder, S.D. Bittencourt, J. Zoppas Ferreira, A.M. Bernardes, Treatment of molybdate solutions by electrodialysis: The effect of pH and current density on ions transport behavior, Separation and Purification Technology. 167 (2016) 32–36. https://doi.org/10.1016/j.seppur.2016.04.047.
[23] J.-H. Choi, S.-H. Moon, Pore size characterization of cation-exchange membranes by chronopotentiometry using homologous amine ions, Journal of Membrane Science. 191 (2001) 225–236. https://doi.org/10.1016/S0376-7388(01)00513-0.
[24] J.-H. Choi, S.-H. Kim, S.-H. Moon, Heterogeneity of Ion-Exchange Membranes: The Effects of Membrane Heterogeneity on Transport Properties, Journal of Colloid and Interface Science. 241 (2001) 120–126. https://doi.org/10.1006/jcis.2001.7710.
[25] S.A. Mareev, D.Yu. Butylskii, N.D. Pismenskaya, V.V. Nikonenko, Chronopotentiometry of ion-exchange membranes in the overlimiting current range. Transition time for a finite-length diffusion layer: modeling and experiment, Journal of Membrane Science. 500 (2016) 171–179. https://doi.org/10.1016/j.memsci.2015.11.026.
[26] I. Rubinstein, B. Zaltzman, T. Pundik, Ion-exchange funneling in thin-film coating modification of heterogeneous electrodialysis membranes, PHYSICAL REVIEW E. (n.d.) 10.
[27] D.Y. Butylskii, S.A. Mareev, N.D. Pismenskaya, P.Y. Apel, O.A. Polezhaeva, V.V. Nikonenko, Phenomenon of two transition times in chronopotentiometry of electrically inhomogeneous ion exchange membranes, Electrochimica Acta. 273 (2018) 289–299. https://doi.org/10.1016/j.electacta.2018.04.026.
[28] E. Volodina, N. Pismenskaya, V. Nikonenko, C. Larchet, G. Pourcelly, Ion transfer across ion-exchange membranes with homogeneous and heterogeneous surfaces, Journal of Colloid and Interface Science. 285 (2005) 247–258. https://doi.org/10.1016/j.jcis.2004.11.017.
[29] M. Persico, S. Mikhaylin, A. Doyen, L. Firdaous, V. Nikonenko, N. Pismenskaya, L. Bazinet, Prevention of peptide fouling on ion-exchange membranes during electrodialysis in overlimiting conditions, Journal of Membrane Science. 543 (2017) 212–221. https://doi.org/10.1016/j.memsci.2017.08.039.
[30] T. Mantel, P. Benne, M. Ernst, Electrically conducting duplex-coated gold-PES-UF membrane for capacitive organic fouling mitigation and rejection enhancement, Journal of Membrane Science. 620 (2021) 118831. https://doi.org/10.1016/j.memsci.2020.118831.
[31] J. Kamcev, R. Sujanani, E.-S. Jang, N. Yan, N. Moe, D.R. Paul, B.D. Freeman, Salt concentration dependence of ionic conductivity in ion exchange membranes, Journal of Membrane Science. 547 (2018) 123–133. https://doi.org/10.1016/j.memsci.2017.10.024.
[32] S.D. Mikhailenko, F. Celso, M.A.S. Rodrigues, S. Kaliaguine, Dielectric Measurements of Polymer Electrolyte Based Composites as a Technique for Evaluation of Membrane Homogeneity, Electrochimica Acta. 136 (2014) 457–465. https://doi.org/10.1016/j.electacta.2014.05.040.
[33] M.-A.D. Paoli, DEGRADAÇÃO E ESTABILIZAÇÃO DE POLÍMEROS, (2008) 228.
[34] W. Garcia-Vasquez, L. Dammak, C. Larchet, V. Nikonenko, N. Pismenskaya, D. Grande, Evolution of anion-exchange membrane properties in a full scale electrodialysis stack,

559 Journal of Membrane Science. 446 (2013) 255–265.
560 https://doi.org/10.1016/j.memsci.2013.06.042.
561 [35] E.D. Belashova, N.D. Pismenskaya, V.V. Nikonenko, P. Sistat, G. Pourcelly, Current-
562 voltage characteristic of anion-exchange membrane in monosodium phosphate solution.
563 Modelling and experiment, Journal of Membrane Science. 542 (2017) 177–185.
564 https://doi.org/10.1016/j.memsci.2017.08.002.
565 [36] V. Sarapulova, E. Nevakshenova, N. Pismenskaya, L. Dammak, V. Nikonenko, Unusual
566 concentration dependence of ion-exchange membrane conductivity in ampholyte-
567 containing solutions: Effect of ampholyte nature, Journal of Membrane Science. 479
568 (2015) 28–38. https://doi.org/10.1016/j.memsci.2015.01.015.
569 [37] K.A. Nebavskaya, V.V. Sarapulova, K.G. Sabbatovskiy, V.D. Sobolev, N.D.
570 Pismenskaya, P. Sistat, M. Cretin, V.V. Nikonenko, Impact of ion exchange membrane
571 surface charge and hydrophobicity on electroconvection at underlimiting and overlimiting
572 currents, Journal of Membrane Science. 523 (2017) 36–44.
573 https://doi.org/10.1016/j.memsci.2016.09.038.
574 [38] G.A. Lindquist, Q. Xu, S.Z. Oener, S.W. Boettcher, Membrane Electrolyzers for Impure-
575 Water Splitting, Joule. 4 (2020) 2549–2561. https://doi.org/10.1016/j.joule.2020.09.020.
576 [39] J. Cheng, G. He, F. Zhang, A mini-review on anion exchange membranes for fuel cell
577 applications: Stability issue and addressing strategies, International Journal of Hydrogen
578 Energy. 40 (2015) 7348–7360. https://doi.org/10.1016/j.ijhydene.2015.04.040.
579 [40] G. Merle, M. Wessling, K. Nijmeijer, Anion exchange membranes for alkaline fuel cells:
580 A review, Journal of Membrane Science. 377 (2011) 1–35.
581 https://doi.org/10.1016/j.memsci.2011.04.043.
582 [41] H.A. Miller, K. Bouzek, J. Hnat, S. Loos, C.I. Bernäcker, T. Weißgärber, L. Röntzsch, J.
583 Meier-Haack, Green hydrogen from anion exchange membrane water electrolysis: a
584 review of recent developments in critical materials and operating conditions, Sustainable
585 Energy Fuels. 4 (2020) 2114–2133. https://doi.org/10.1039/C9SE01240K.
586 [42] V.I. Zabolotsky, V.V. Nikonenko, Effect of structural membrane inhomogeneity on
587 transport properties, Journal of Membrane Science. 79 (1993) 181–198.
588 https://doi.org/10.1016/0376-7388(93)85115-D.
589 [43] G.Yu. Lopatkova, E.I. Volodina, N.D. Pis'menskaya, Yu.A. Fedotov, D. Cot, V.V.
590 Nikonenko, Effect of chemical modification of ion-exchange membrane MA-40 on its
591 electrochemical characteristics, Russian Journal of Electrochemistry. 42 (2006) 847–854.
592 https://doi.org/10.1134/S1023193506080064.
593 [44] N.D. Pismenskaya, E.V. Pokhidnia, G. Pourcelly, V.V. Nikonenko, Can the
594 electrochemical performance of heterogeneous ion-exchange membranes be better than
595 that of homogeneous membranes?, Journal of Membrane Science. 566 (2018) 54–68.
596 https://doi.org/10.1016/j.memsci.2018.08.055.
597 [45] L. Wang, Z. Li, Z. Xu, F. Zhang, J.E. Efome, N. Li, Proton blockage membrane with
598 tertiary amine groups for concentration of sulfonic acid in electrodialysis, Journal of
599 Membrane Science. 555 (2018) 78–87. https://doi.org/10.1016/j.memsci.2018.03.011.
600 [46] N. Pismenskaia, P. Sistat, P. Huguet, V. Nikonenko, G. Pourcelly, Chronopotentiometry
601 applied to the study of ion transfer through anion exchange membranes, Journal of
602 Membrane Science. 228 (2004) 65–76. https://doi.org/10.1016/j.memsci.2003.09.012.
603 [47] K.S. Barros, M.C. Martí-Calatayud, E.M. Ortega, V. Pérez-Herranz, D.C.R. Espinosa,
604 Chronopotentiometric study on the simultaneous transport of EDTA ionic species and
605 hydroxyl ions through an anion-exchange membrane for electrodialysis applications,
606 Journal of Electroanalytical Chemistry. 879 (2020) 114782.
607 https://doi.org/10.1016/j.jelechem.2020.114782.

[48] C. Gally, M. García-Gabaldón, E.M. Ortega, A.M. Bernardes, V. Pérez-Herranz, Chronopotentiometric study of the transport of phosphoric acid anions through an anion-exchange membrane under different pH values, Separation and Purification Technology. 238 (2020) 116421. https://doi.org/10.1016/j.seppur.2019.116421.
[49] S.A. Mareev, A.V. Nebavskiy, V.S. Nichka, M.Kh. Urtenov, V.V. Nikonenko, The nature of two transition times on chronopotentiograms of heterogeneous ion exchange membranes: 2D modelling, Journal of Membrane Science. 575 (2019) 179–190. https://doi.org/10.1016/j.memsci.2018.12.087.
[50] R.K. Nagarale, V.K. Shahi, S.K. Thampy, R. Rangarajan, Studies on electrochemical characterization of polycarbonate and polysulfone based heterogeneous cation-exchange membranes, Reactive and Functional Polymers. 61 (2004) 131–138. https://doi.org/10.1016/j.reactfunctpolym.2004.04.007.
[51] D.-H. Kim, J.-H. Park, S.-J. Seo, J.-S. Park, S. Jung, Y.S. Kang, J.-H. Choi, M.-S. Kang, Development of thin anion-exchange pore-filled membranes for high diffusion dialysis performance, Journal of Membrane Science. 447 (2013) 80–86. https://doi.org/10.1016/j.memsci.2013.07.017.
[52] M.C. Martí-Calatayud, D.C. Buzzi, M. García-Gabaldón, A.M. Bernardes, J.A.S. Tenório, V. Pérez-Herranz, Ion transport through homogeneous and heterogeneous ion-exchange membranes in single salt and multicomponent electrolyte solutions, Journal of Membrane Science. 466 (2014) 45–57. https://doi.org/10.1016/j.memsci.2014.04.033.
[53] N.D. Pismenskaya, V.V. Nikonenko, N.A. Melnik, K.A. Shevtsova, E.I. Belova, G. Pourcelly, D. Cot, L. Dammak, C. Larchet, Evolution with Time of Hydrophobicity and Microrelief of a Cation-Exchange Membrane Surface and Its Impact on Overlimiting Mass Transfer, The Journal of Physical Chemistry B. 116 (2012) 2145–2161. https://doi.org/10.1021/jp2101896.
[54] T. Belloň, Z. Slouka, Overlimiting behavior of surface-modified heterogeneous anion-exchange membranes, Journal of Membrane Science. (2020) 118291. https://doi.org/10.1016/j.memsci.2020.118291.
[55] N.P. Berezina, N.A. Kononenko, O.A. Dyomina, N.P. Gnusin, Characterization of ion-exchange membrane materials: Properties vs structure, Advances in Colloid and Interface Science. 139 (2008) 3–28. https://doi.org/10.1016/j.cis.2008.01.002.
[56] V.V. Nikonenko, N.D. Pismenskaya, E.I. Belova, P. Sistat, P. Huguet, G. Pourcelly, C. Larchet, Intensive current transfer in membrane systems: Modelling, mechanisms and application in electrodialysis, Advances in Colloid and Interface Science. 160 (2010) 101–123. https://doi.org/10.1016/j.cis.2010.08.001.
[57] O. Rybalkina, K. Tsygurina, E. Melnikova, S. Mareev, I. Moroz, V. Nikonenko, N. Pismenskaya, Partial Fluxes of Phosphoric Acid Anions through Anion-Exchange Membranes in the Course of NaH2PO4 Solution Electrodialysis, IJMS. 20 (2019) 3593. https://doi.org/10.3390/ijms20143593.
[58] V.I. Vasil'eva, N.A. Kranina, M.D. Malykhin, E.M. Akberova, A.V. Zhiltsova, The surface inhomogeneity of ion-exchange membranes by SEM and AFM data, J. Synch. Investig. 7 (2013) 144–153. https://doi.org/10.1134/S1027451013010321.
[59] D. Ariono, Khoiruddin, Subagjo, I.G. Wenten, Heterogeneous structure and its effect on properties and electrochemical behavior of ion-exchange membrane, Mater. Res. Express. 4 (2017) 024006. https://doi.org/10.1088/2053-1591/aa5cd4.
[60] L. Dammak, C. Larchet, D. Grande, Ageing of ion-exchange membranes in oxidant solutions, Separation and Purification Technology. 69 (2009) 43–47. https://doi.org/10.1016/j.seppur.2009.06.016.
[61] V. Bhadja, B.S. Makwana, S. Maiti, S. Sharma, U. Chatterjee, Comparative Efficacy Study of Different Types of Ion Exchange Membranes for Production of Ultrapure Water

via Electrodeionization, Ind. Eng. Chem. Res. 54 (2015) 10974–10982. https://doi.org/10.1021/acs.iecr.5b03043.
[62] M.M. Seepana, J. Pandey, A. Shukla, Synthesis and characterization of PWA based inorganic ion-exchange membrane, Separation and Purification Technology. 98 (2012) 193–198. https://doi.org/10.1016/j.seppur.2012.07.012.
[63] P. Knauth, H. Hou, E. Bloch, E. Sgreccia, M.L. Di Vona, Thermogravimetric analysis of SPEEK membranes: Thermal stability, degree of sulfonation and cross-linking reaction, Journal of Analytical and Applied Pyrolysis. 92 (2011) 361–365. https://doi.org/10.1016/j.jaap.2011.07.012.
[64] A.E. Kozmai, V.V. Nikonenko, S. Zyryanova, N.D. Pismenskaya, L. Dammak, A simple model for the response of an anion-exchange membrane to variation in concentration and pH of bathing solution, Journal of Membrane Science. 567 (2018) 127–138. https://doi.org/10.1016/j.memsci.2018.07.007.
[65] J.-H. Tay, J. Liu, D.D. Sun, Quantification of membrane fouling using thermogravimetric method, Journal of Membrane Science. 217 (2003) 17–28. https://doi.org/10.1016/S0376-7388(02)00554-9.
[66] J. Parrondo, C. G. Arges, M. Niedzwiecki, E. B. Anderson, K. E. Ayers, V. Ramani, Degradation of anion exchange membranes used for hydrogen production by ultrapure water electrolysis, RSC Advances. 4 (2014) 9875–9879. https://doi.org/10.1039/C3RA46630B.
[67] H. Zarrin, J. Fu, G. Jiang, S. Yoo, J. Lenos, M. Fowler, Z. Chen, Quaternized Graphene Oxide Nanocomposites as Fast Hydroxide Conductors, ACS Nano. 9 (2015) 2028–2037. https://doi.org/10.1021/nn507113c.
[68] A.D. Mohanty, S.E. Tignor, J.A. Krause, Y.-K. Choe, C. Bae, Systematic Alkaline Stability Study of Polymer Backbones for Anion Exchange Membrane Applications, Macromolecules. 49 (2016) 3361–3372. https://doi.org/10.1021/acs.macromol.5b02550.
[69] Z. Yang, J. Ran, B. Wu, L. Wu, T. Xu, Stability challenge in anion exchange membrane for fuel cells, Current Opinion in Chemical Engineering. 12 (2016) 22–30. https://doi.org/10.1016/j.coche.2016.01.009.